Langmuir
Article
pubs.acs.org/Langmuir

Formation of Magnesium Fluoride Particles of Different Morphologies

Igor Sevonkaev and Egon Matijević*

Center for Advanced Materials processing, Clarkson University, Potsdam, New York 13699-5814

Received April 13, 2009. Revised Manuscript Received May 18, 2009

Uniform dispersions of magnesium fluoride particles of different morphologies were prepared by precipitation in aqueous solutions. The resulting cubic, prismatic, and platelet-like nanosize solids had single crystal structure with X-ray pattern characteristic of the mineral sellaite. In contrast, two kinds of polycrystalline MgF_2 spheres were obtained by aggregation of the nanosize subunits. The mechanisms of the formation of the resulting particles of different shapes are explained by the role of the pH and ionic strength. In addition, for prospective numerical modeling the surface tension of spherical and platelet particles of MgF_2 was evaluated from the X-ray data by a lattice parameter change method.

1. Introduction

It is well-known that many properties of finely dispersed matter depend on the size and shape of individual particles of the same chemical composition. To evaluate these effects, it is necessary to deal with well-defined dispersions of fine particles. While different techniques have been used in the preparation of uniform particles, the precipitation in homogeneous solutions is advantageous, because of the experimental simplicity and versatility. The comprehensive volume, edited by Sugimoto,[1] describes many such simple and composite finely dispersed matter of various shapes, modal sizes, and different structures.

While the progress in the ability to obtain these materials is quite impressive, much less successful have been efforts to elucidate the mechanisms of their formation. As a result, the preparation of dispersions of specific chemical and physical characteristics still depends, to a great extant, on the skills of the experimentalists. The reason for this uncertainty is easily understood, because the properties of precipitated products are affected in a sensitive way on the complexation of the reactants in the liquid media. The latter may vary with the experimental parameters, including the concentration, solubility, pH, temperature, aging, and additives (such as stabilizers), all of which also depend on the solvent used.

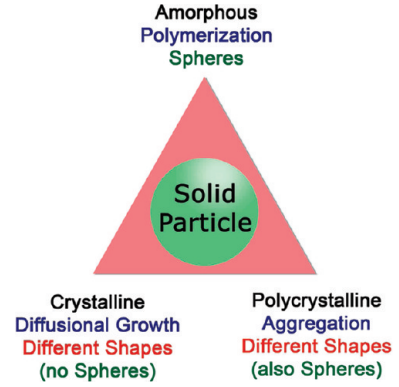

Figure 1. 0Schematic classification of mechanisms of particles formation.

By considering a large number of reported "monodispersed" colloids,[2−16] and taking into account specific preparation conditions, a general classification of mechanisms of particle formations was proposed,[17] which is schematically given in Figure 1.

The top of the triangle represents processes in which the particles are formed by polymerization of solute monomers, as in the example of silica, produced by condensation of silicic acid molecules. In such cases, the resulting particles are, as a rule, amorphous spheres. The left side of the triangle refers to the formation of particles by diffusion of constituent solutes onto nuclei. These precipitates appear as crystals of different shapes, except spherical, and can be uniform under certain conditions.

Finally, the right-hand side of the scheme refers to the mechanism, by which the final particles are made of small (nanosize) entities, which are formed first and subsequently aggregate to a larger size.[17−20] This process can yield uniform particles of different shapes including spheres. There is ample

*matiegon@clarkson.edu.

(1) Sugimoto *Fine Particles Synthesis, Characterization, and Mechanism of Growth*, 1st ed.; Marcel Dekker: New York, 2000.
(2) Botella, P.; Corma, A.; Navarro, M. T. *Chem. Mater.* **2007**, *19*, 1979–1983.
(3) Camargo, P. H. C.; Li, Z. Y.; Xia, Y. *Soft Matter* **2007**, *3*, 1215–1222.
(4) Cho, Y. S.; Yi, G. R.; Chung, Y. S.; Bin Park, S.; Yang, S. M. *Langmuir* **2007**, *23*, 12079–12085.
(5) Chung, Y. W.; Leu, I. C.; Lee, J. H.; Hon, M. H. *Colloids Surf., A* **2006**, *290*, 256–262.
(6) Elechiguerra, J. L.; Larios-Lopez, L.; Jose-Yacaman, M. *Appl. Phys. A: Mater. Sci. Process.* **2006**, *84*, 11–19.
(7) Huang, W. H.; Li, J. A.; Xue, L. J.; Xing, R. B.; Luan, S. F.; Luo, C. X.; Liu, L. B.; Han, Y. C. *Colloids Surf., A* **2006**, *278*, 144–148.
(8) Luo, Y. L. *Colloid J.* **2007**, *69*, 391−393.
(9) Nakamura, T.; Yamada, Y.; Yano, K. *J. Mater. Chem.* **2006**, *16*, 2417–2419.
(10) Nguyen, H. L.; Howard, L. E. M.; Giblin, S. R.; Tanner, B. K.; Terry, I.; Hughes, A. K.; Ross, I. M.; Serres, A.; Burckstummer, H.; Evans, J. S. O. *J. Mater. Chem.* **2005**, *15*, 5136–5143.
(11) Panda, S. K.; Datta, A.; Chaudhuri, S. *Chem. Phys. Lett.* **2007**, *440*, 235–238.
(12) Tzitzios, V. K.; Georgakilas, V.; Niarchos, D.; Petridis, D. *J. Nanosci. Nanotechnol.* **2006**, *6*, 2081–2083.
(13) Wang, H. H.; Xie, C. S.; Zeng, D. W.; Yang, Z. H. *J. Colloid Interface Sci.* **2006**, *297*, 570–577.
(14) Wyrwa, D. W.; Schmid, G. J. *Cluster Sci.* **2007**, *18*, 476–493.
(15) Zhong, H. Z.; Wei, Z. X.; Ye, M. F.; Yan, Y.; Zhou, Y.; Ding, Y. Q.; Yang, C. H.; Li, Y. F. *Langmuir* **2007**, *23*, 9008–9013.
(16) Zhu, Y. F.; Zhao, W. R.; Chen, H. R.; Shi, J. L. *J. Phys. Chem. C* **2007**, *111*, 5281–5285.
(17) Matijević, E.; Goia, D. *Croat. Chem. Acta* **2007**, *80*, 485–491.
(18) Matijević, E. *Chem. Mater.* **1993**, *5*, 412–426.
(19) Park, J.; Privman, V.; Matijević, E. *J. Phys. Chem. B* **2001**, *105*, 11630–11635.
(20) Matijević, E. *Colloid J.* **2007**, *69*, 29–38.

Table 1. Initial Experimental Conditions (Volumes, Concentrations, and pH) and Resulting Morphologies of MgF_2 Particles[a]

	Initial conditions of stock solutions							
	NaF		$MgCl_2$		$MgAc_2$			
#	C, mol/dm^3	V, cm^3	C, mol/dm^3	V, cm^3	C, mol/dm^3	V, cm^3	pH	results
A_1	0.02	10	0.2	10	—	—	11 (NaOH)	Platelet particles (Figure 2)
A_2	0.02	10	—	—	0.2	10	11 (NaOH)	
A_3	0.02	10	0.2	10	—	—	11 (LiOH)	
A_4	0.02	10	—	—	0.2	10	11 (LiOH)	
B_1	0.02	10	0.2	10	—	—	6	Cubic particles (Figure 3)
B_2	0.01	10	0.1	10	—	—	6	
C	0.02	10	0.2	10	—	—	2.7 (HCl)	Rectangular particles (Figure 4)
D_1	0.2	10	0.2	10	—	—	6	Polycrystalline spherical particles[25,26] (Figure 5)
D_2	0.1	10	0.1	10	—	—	6	
E_1	0.02	10	—	—	0.2	10	6	Polycrystalline spherical particles (Figure 6)
E_2	0.01	10	—	—	0.1	10	6	

[a] All reactions were carried out at 80 °C.

experimental evidence demonstrating that great many dispersions of larger particles are formed by this process.

It is, therefore, of interest to further investigate the multistage growth mechanism, as it can yield particles of any shape. It is also an intriguing task to explain how countless small precursors can form identical large particles of a given shape. A model, which accounts for the formation of uniform spheres by aggregation, was developed and successfully tested for dispersions of metals and salts.[18,21−24] Still, the size selection of particles of different shapes by aggregation remains an unresolved problem, presenting many challenges. To understand these complex issues, it is desirable to obtain experimental data on solids of simple chemical composition. It is also important that constituent ions show little tendency for complexion in reacting solution and yield uniform particles of well-defined shapes.

This study, dealing with MgF_2 particles, fulfills the described conditions. The constituent ions (F^-, Mg^{2+}) do not form complexes in aqueous solutions (except Mg^{2+} at higher pH), and the final product has a rather simple crystalline structure. Furthermore, depending on the experimental conditions, the particles may appear in different shapes (spherical, cubic, prismatic, or plate-like), by mechanisms given in Figure 1.

2. Experimental Section

2.1. Preparation Method. The particles used in this study were prepared by precipitation in aqueous solutions of NaF and $MgCl_2$. Specifically, salt solutions were preheated to 80 °C, rapidly combined in equal volumes of various predetermined concentrations, and then aged in a thermostatted water bath at the same temperature. Preliminary experiments were carried out to follow the growth of precipitated particles by removing samples over a 5 h period. These samples were examined by electron microscopy to observe any changes in particle properties with time. It was established that the precipitates formed almost instantaneously and no changes were observed after 2 h of aging. Therefore, as a rule solids generated after 2 h were removed by filtration, washed on a General Electric (GE) polycarbonate membrane, and subsequently dried in vacuum. Further evaluations showed that the methods of cooling and drying particles had no noticeable effect on their size and shape.

Additional tests were carried out to establish effects of various anions and of the pH on the final precipitates. In the former case, magnesium chloride salt was substituted by magnesium acetate, while the pH effect was tested by adding either a base (NaOH or LiOH) or an acid (HCl), while keeping all other conditions unchanged. The experimental parameters for all systems are summarized in Figure 1.

2.2. Materials and Characterization. All reactants were of the highest purity grade. The resulting particles were inspected by transmission (TEM, JEM-2010) and scanning (FESEM, JEOL-7400) electron microscopes. The structure of the particles was evaluated by electron diffraction (JEM-2010) and X-ray diffraction (XRD, Bruker-AXS D8 Focus). The chemical composition of the solids was qualitatively assessed by energy dispersive spectroscopy (EDS, JEOL JSM-6300). Size distribution of the dispersions and zeta potentials were determined by light scattering (Brookhaven ZetaPlus/90Plus). The presence of any precipitates was detected by passing laser beam through the solution (Tyndall effect).

For electron microscopy observations, particles were redispersed in deionized water, a drop of the dispersion was placed on a grid or a stub, and then the liquid was removed with a capillary after the solids were allowed to settle.

For XRD analysis, a sufficient amount of the powder was dried and packed onto a sample holder. Typical scan parameters were set as follows: step width, 0.01°; step period, 5 s. Source, sample, and detector slits were 2, 0.6, and 1 mm, respectively.

3. Results

Depending on the experimental conditions, either crystalline particles of various morphologies or polycrystalline spheres were obtained, as two cases given at the bottom of the scheme (Figure 1). No amorphous solids precipitated, because Mg^{2+} and F^- ions do not tend to form polymeric complexes in solution. Earlier,[25,26] it was demonstrated that mixing solutions of $MgCl_2$ and NaF yielded dispersions of either spherical MgF_2 (sellaite) or cubic $NaMgF_3$ (neighborite) particles. In the present, more detailed study, it has been found that at lower concentrations of reactants only MgF_2 of various morphologies can be obtained.

3.1. Nonspherical MgF_2 Crystalline Particles of Different Morphologies. One of the essential parameters that influenced the morphology of these crystalline particles was the pH of reactant solutions. By varying this parameter, uniform finely dispersed solids of platelet-type, cubic, or prismatic shapes were obtained.

Preparation of MgF_2 Platelets. Precipitation at pH 11 (adjusted either with NaOH or LiOH) yielded MgF_2 platelet-type particles by mixing NaF with either $MgCl_2$ or $MgAc_2$

(21) Privman, V.; Goia, D.; Park, J.; Matijević, E. *J. Colloid Interface Sci.* **1999**, *213*, 36–45.
(22) Libert, S.; Gorshkov, V.; Privman, V.; Goia, D.; Matijevic, E. *LANL Preprint Archive, Cond. Matter* **2002**, *1*, 18.
(23) Libert, S.; Goia, D.; Matijević, E. *Langmuir* **2003**, *19*, 10673–10678.
(24) Libert, S.; Gorshkov, V.; Goia, D.; Matijević, E.; Privman, V. *Langmuir* **2003**, *19*, 10679–10683.
(25) Hsu, W. P.; Zhong, Q.; Matijević, E. *J. Colloid Interface Sci.* **1996**, *181*, 142–U148.
(26) Sevonkaev, I.; Goia, D.; Matijević, E. *J. Colloid Interface Sci.* **2008**, *317*, 130–136.

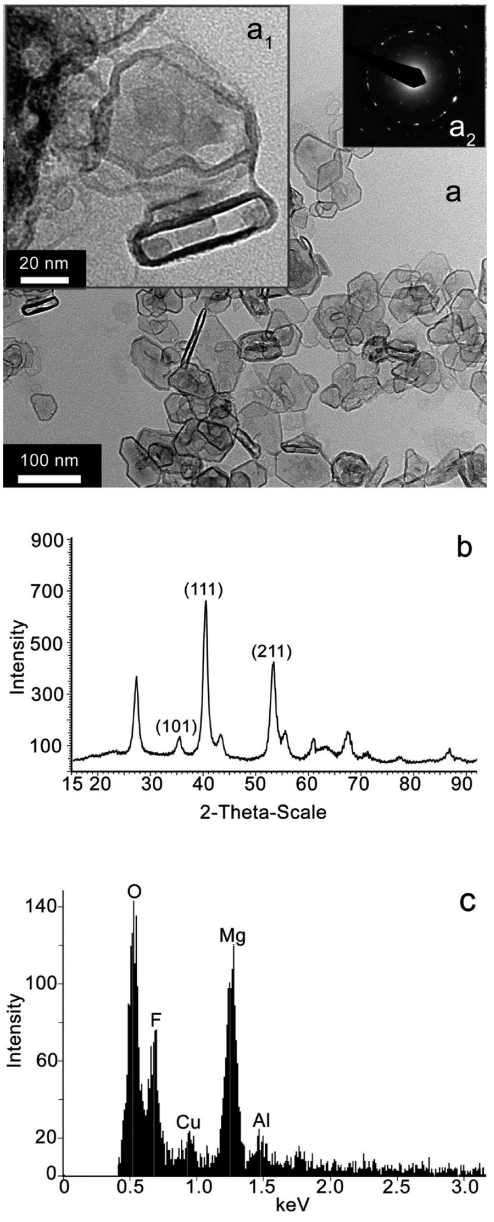

Figure 2. Platelet-type MgF_2 particles obtained under conditions in Table 1A. (a) Platelet crystals, (a_1) two magnified platelets in different orientations, (a_2) their electron diffraction; (b) X-ray diffractogram; and (c) EDX pattern.

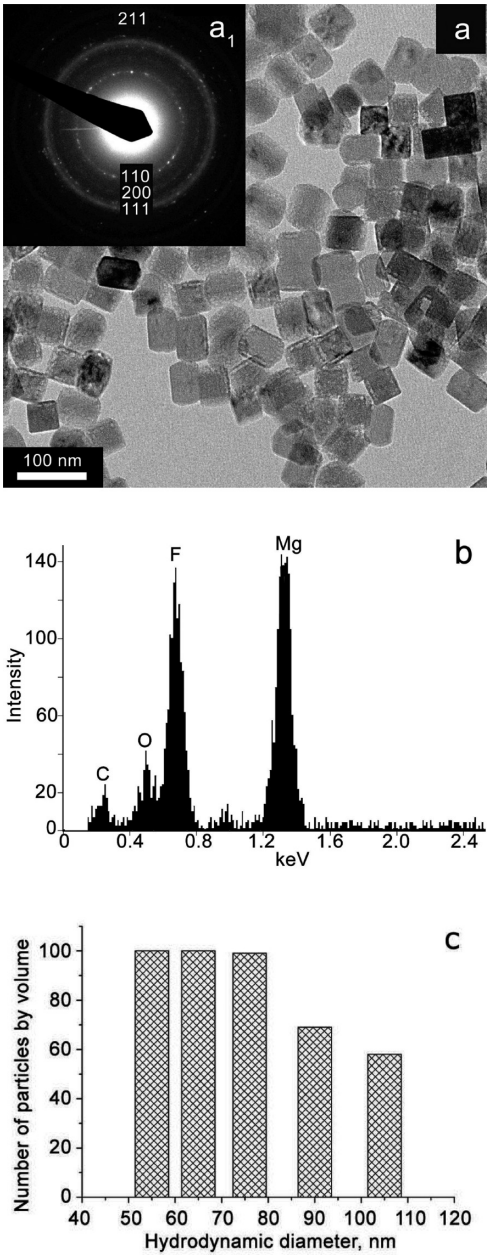

Figure 3. Cubic MgF_2 particles obtained under conditions in Table 1B. (a) TEM image and (a_1) electron diffraction of cubic crystals; (b) EDX spectrum; (c) corresponding size distribution.

(Table 1,A_1−A_4). In order to prevent precipitation of $Mg(OH)_2$, three aqueous solutions were prepared ($MgCl_2$ or $MgAc_2$, NaF, and NaOH or LiOH). The solutions of NaF and the base were combined first, and then mixed with the magnesium salt solution. In all four cases, precipitation occurred rapidly (in less than a minute), as observed by the Tyndall effect.

The electron micrograph in Figure 2a displays the resulting platelets, which are 100−150 mn wide and 10−20 nm thick. Identical results were obtained with both magnesium salts, as well as by adjusting the pH with either base. The X-ray diffraction in Figure 2b is characteristic of the MgF_2 mineral sellaite. The inserted electron diffractogram is indicative of their single crystalline nature. The composition of these particles was also corroborated by the EDX analysis (Figure 2c).

Preparation of MgF_2 Cubes. By mixing aqueous solutions of $MgCl_2$ and NaF at pH 6 without any additives (base or acid) under conditions in Table 1, B produced single crystal cubes of MgF_2 (Figure 3a). The corresponding electron diffraction ($3a_1$) and EDX (Figure 3b) confirmed the structure and the chemical composition of the solids. The typical, positively skewed size distribution of such a dispersion is illustrated in Figure 3c. Changing the concentration of $MgCl_2$ in the range given in Table 1, B did not affect the characteristics of these particles. However, substituting $MgCl_2$ with $MgAc_2$ resulted in different products, which will be described in the next section.

Preparation of MgF_2 Prismatic Particles. Mixing NaF and $MgCl_2$ at pH 2.7 (adjusted with HCl, 1, C) yielded prismatic particles illustrated in Figure 4a. In this case, it took a somewhat longer time (~5 min) for the particles to form (as indicated by the Tyndall effect) than what was observed in the cases of platelets and cubes. The resulting particles of ~500−600 nm in length and 300−400 nm thickness eventually settled down. The EDX

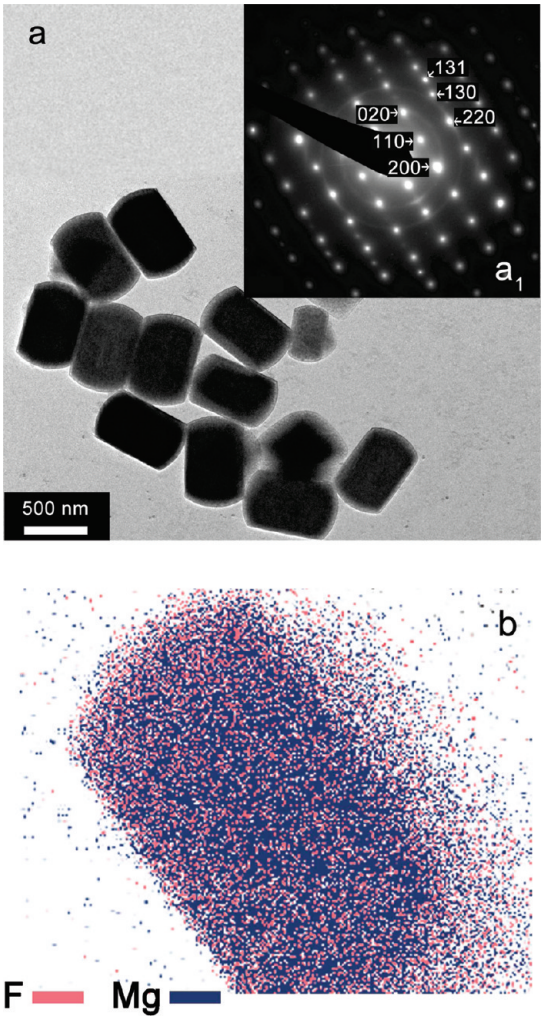

Figure 4. Prismatic MgF_2 particles obtained under conditions in Table 1C. (a) TEM image, (a_1) electron diffraction of a single particle; (b) element mapping in scanning TEM mode indicates only magnesium and fluorine.

mapping (Figure 4b) confirms only the presence of Mg and F and the electron diffraction pattern their sellaite structure ($4a_1$).

3.2. Polycrystalline Spherical MgF_2 Particles. Two distinct types of spherical particles were obtained under conditions specified in Table 1, D and E. Earlier,[26] uniform MgF_2 spherical particles made of nanosubunits were obtained under conditions in Table 1, D. Samples taken approximately every 10−15 min during a subsequent aging period of 1 h showed that spheres grew slightly with time. The X-ray diffraction pattern of the solids is characteristic of MgF_2 (Figure 5b). Furthermore, the XRD data confirmed the composite internal structure of those particles, consisting of subunits of 5−15 nm in diameter, as derived by the Scherrer method.[27] The chemical composition was corroborated by EDX analysis, which detected only Mg and F elements.

In this study, spherical sellaite particles were obtained, when $MgAc_2$ was used instead of $MgCl_2$ (Table 1, E). The size distribution of these spheres, determined by light scattering (Figure 6d), shows them to be polydisperse with a modal diameter of 270 ± 50 nm, a value which is consistent with electron microscopy observations. Electron micrographs in bright (Figure 6a,b) and dark field (Figure 6c) reveal internal composition of the spheres

(27) Patterson, A. L. *Phys. Rev.* **1939**, *56*, 978–982.

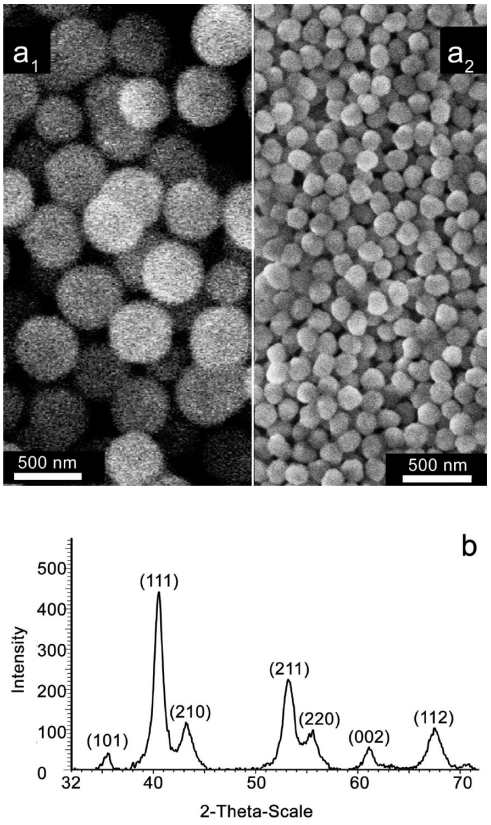

Figure 5. (a) Spherical polycrystalline particles obtained under conditions in Table 1D of two different sizes;[25,26] (b) their X-ray diffraction.

made of somewhat loosely packed subunits of ∼50 nm. The EDX analysis confirmed crystallites to be pure MgF_2.

3.3. Surface Tension of Magnesium Fluoride Nanoparticles. Surface tension is one of the important experimental parameters needed in an effort to elucidate the mechanisms of the formation of fine particles. It was shown[28,29] that surface tension of solids is the tangential stress in the surface layer, which is characteristics of microcrystals and diminishes as the crystallites grow. Therefore, surface tension σ in microcrystals, as it was shown by Nicolson[29] and later refined by Stoneham,[30] may be measured by lattice parameter change and expressed with good accuracy for particles of different shapes by

$$\sigma = -3\Delta a/4\beta \qquad (1)$$

where β is the compressibility and Δa absolute change in lattice parameter.

The surface tension of MgF_2 microcrystalline platelets (Figure 2b) and spherical (Figure 5b) particles was assessed from X-ray diffraction data. According to Equation 1, it is necessary to have exact values of lattice parameters and compressibility of the investigated material. Values for the latter were taken from Haines study.[31] For precise peaks characteristics, diffractograms were refined in the *Topaz* software package and then processed with the use of the Nelson−Riley function ($\cos^2\theta/\sin\theta + \cos 2\theta/\theta$) for exact values of lattice parameters a and c. Deviation of

(28) Shuttleworth, R. *Proc. Phys. Soc. London, Sect. A* **1950**, *63*, 444–457.
(29) Nicolson, M. M. *Proc. R. Soc. London, Ser. A* **1955**, *228*, 490–510.
(30) Stoneham, A. M. *J. Phys. C: Solid State Phys.* **1977**, *10*, 1175–1179.
(31) Haines, J.; L'eger, J. M.; Gorelli, F.; Klug, D. D.; Tse, J. S.; Li, Z. Q. *Phys. Rev. B* **2001**, *64*, 134110.

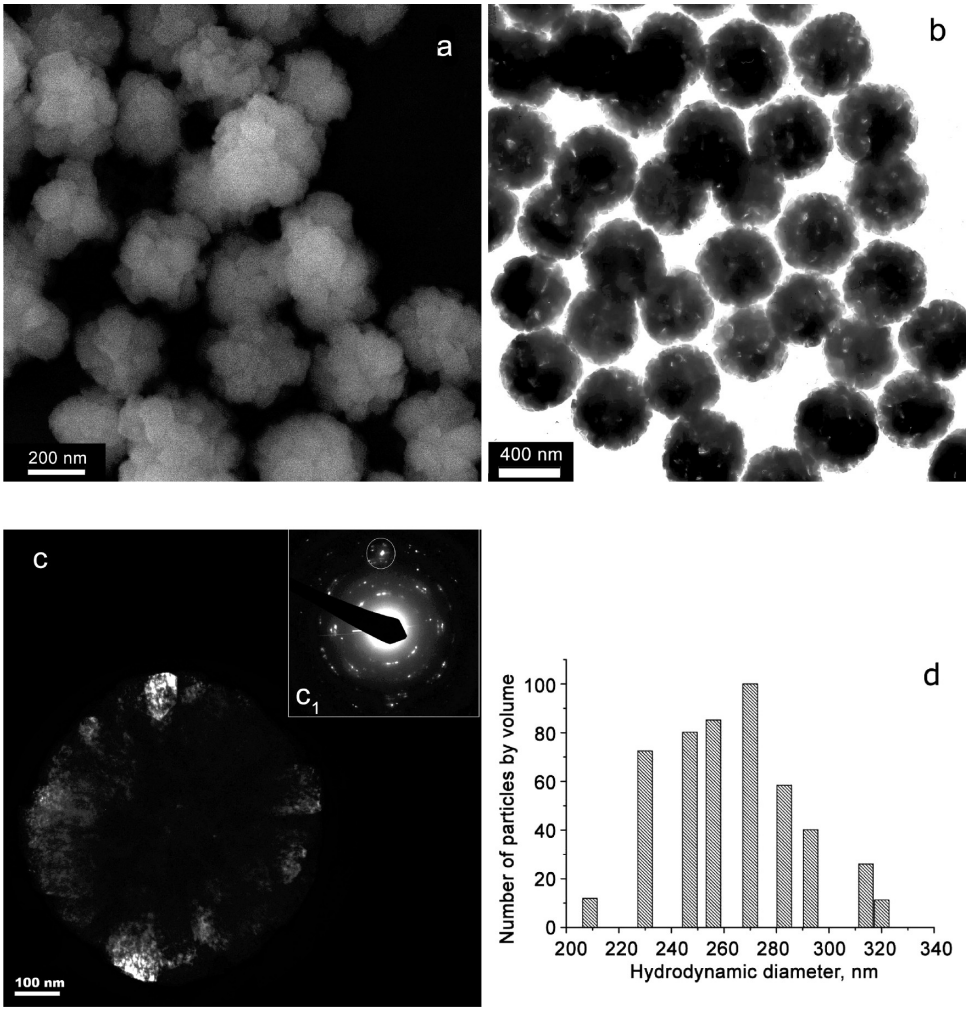

Figure 6. (a) SEM and (b) TEM images of spherical particles obtained under conditions in Table 1E. (c) Dark field image of a single particle, with (c_1) corresponding electron diffraction; (d) size distribution of these particles obtained by light scattering.

the lattice parameters from those reported for the bulk crystals[32] amounted to $\Delta a_{\text{spheres}} = 1.558 \times 10^{-1}$ Å and $\Delta a_{\text{spheres}} = 1.284 \times 10^{-1}$ Å, and $\Delta a_{\text{spheres}} = 8 \times 10^{-4}$ Å and $\Delta a_{\text{platelets}} = 4.38 \times 10^{-2}$ Å. The above data, summarized in Table 2, yielded surface tensions.

4. Discussion

This study has shown that by using the same reactants one may precipitate particles of the same chemical composition by different mechanisms, resulting in a variety of morphologies. Specifically, by changing experimental parameters, such as the pH and the ionic strength, MgF_2 was prepared as uniform crystals of different habitus or as polycrystalline spheres. These particles form by different mechanisms classified at the bottom side of the triangle shown in Figure 1.

4.1. Crystalline Particles. Crystalline particles of platelet, cubic, or prismatic shapes, obtained by changing the pH, were formed by diffusional growth (left corner of the scheme). MgF_2 cubes, ranging in size from 50 to 100 nm and having the X-ray diffraction pattern of the mineral sellaite, precipitated under essentially neutral conditions (Table 1, B). The skewed shape of their size distribution (Figure 3c) is indicative of the diffusional growth mechanism, as modeled by Privman.[33] Under certain conditions, as explained below in this section, these particles may aggregate to form polycrystalline spheres.

The ξ-potential of cubic particles, purified by extensive washing and redispersed in pure water, was 64 ± 10 mV and their isoelectric point (IEP) was estimated between pH 8 and 9.5. Thus, cubic particles grew at the pH below the IEP, resulting in the positive charge due to the specific adsorption of Mg^{2+}.

Prismatic $\sim 600 \times 400$ nm^2 single crystals of MgF_2 were formed at acidic conditions (sample C), below the IEP analogously to the previous case. Due to a higher solubility of MgF_2 under such conditions, the supersaturation lower than in neutral and basic solutions was responsible for slower crystal growth, resulting in larger elongated particles. Resolved electron diffraction confirmed sellaite crystal structure, and the EDX mapping indicated only Mg and F constituents (Figure 4b).

In contrast to the previous two cases, thin MgF_2 hexagonal platelets were formed above the IEP in basic solutions (LiOH or NaOH, pH 11). Using values for the solubility products of MgF_2 ($K_{sp} = 5.16 \times 10^{-11}$)[34] and of $Mg(OH)_2$ ($K_{sp} = 5.61 \times 10^{-12}$),[34] and taking into account concentrations of the reactants (Table 1, A), sellaite should preferentially precipitate. Indeed, electron diffraction and powder X-ray diffraction (Figure 2b) did not

(32) Vidal-Valat, G.; Vidal, J.-P.; Zeyen, C. M. E.; Kurki-Suonio, K. *Acta Crystallogr., Sect. B* **1979**, *35*, 1584–1590.
(33) Privman, V. J. *Optoelectronics Adv. Mater.* **2008**, *10*, 2827–2839.
(34) *CRC Handbook of Chemistry and Physics*, 79th ed.; Lide, D. R., Ed.; CRC Press: Boca Raton, 1999.

Table 2. Surface Tension of MgF_2 Particles of Different Shapes Calculated with the Values of Parameters in eq 1

	LP[a]	MgF_2 spheres	MgF_2 platelets
sample		D	A
micrograph		Figure 5a	Figure 2a
XRD		Figure 5b	Figure 2b
lattice parameters for bulk crystal[32] Å	*a*	4.6280	
	c	3.0450	
lattice parameters, obtained from experiment by Nelson-Riley approximation, Å	*a*	4.5875	4.6288
	c	3.0937	3.0889
compressibility,[31] GPa^{-1}	*a*	0.003	
	c	0.0024	
absolute values of surface tension, N/m	*a*	3.89	0.02
	c	4.01	1.37

[a] Lattice parameter.

detect any possible hydroxy compounds, such as $Mg(OH)_2$, Mg(OH)F, or Mg(OH)Cl. EDX, however, detected some oxygen in all samples A_1-A_4 (Table 1), which indicates some adsorption of the OH^- group on the surface of the platelets, as is also indicated by the lower value of the electrokinetic potential ($\xi = 30 \pm 3$ mV) as compared to cubes. Hexagonal shape of the plates and their preferential growth in two dimensions lead to the conclusion that these hydroxyl ions are bound on the (111) face of the nuclei, preventing growth in the direction perpendicular to that face.

Another correlation between different MgF_2 crystal shapes was found by considering the surface tension data (Table 2), which show that in the case of platelets *c* lattice parameter was significantly more stressed than *a*, resulting in free crystal growth in the *XY* plane and suppressed growth in the *Z* direction (Figure 2a).

4.2. Polycrystalline Particles. Two different samples of polycrystalline MgF_2 spheres were obtained, as classified in the right corner of the scheme (Figure 1). The formation of aggregated particles, displayed in Figure 5a, is caused by sufficiently high ionic strength. Under conditions in Table 1, D, the resulting spheres consisted of nanosize precursors of 5−15 nm in size, assessed from the broadening of the X-ray peaks by the Scherrer method.[27] Such crystallites uniformity was expected considering their almost identical lattice parameter stresses (Table 2). Similar cases have been observed before with metallic particles (Ag,[35,36] Au[36]) and inorganic salt particles (CdS[24]). A model, describing conditions leading to uniform spheres by such aggregation, has been successfully tested on the cited systems.

Somewhat different conditions are encountered in polycrystalline spheres displayed in Figure 6a, which consist of cubic subunits (similar to sample B). Symmetrical size distribution profile of the spherical particles (sample E, Figure 6d) and loose packing of the cubic subunits (which can be seen in bright and in dark field TEM images as transparent areas inside individual aggregates in Figure 6a−c) suggest slow aggregation of crystallites into larger spherical particles. The number of such subunits in each aggregate was estimated to be roughly between 13 and 30. The unique aspect of this system is that the aggregation of the subunits is only observed when magnesium acetate (rather than $MgCl_2$) was used as a reactant in the precipitation process. Consequently, one needs to speculate on the role of acetate rather than chloride anions in this particular case. Since the reactant concentrations and all other conditions were the same as those in sample B, the adsorbability, size, and shape of the acetate ion must have an effect on the aggregation process. While the ξ-potential for particles prepared with acetate ion was, as a rule, lower by 10 mV than the value obtained with Cl^-, this difference is not sufficient to account for lesser stability of the precursors. A possible explanation may be based on the adsorption of acetate ions, which would certainly involve carboxyl group attachment to magnesium sites on the particles surfaces and, consequently, tail-to-tail interaction of the approaching subunits.

5. Conclusion

This study illustrates the complexity of the problems related to the preparation, in a predictable way, of uniform particles of a given chemical composition and shape by the precipitation process. Using a system of a relatively simple chemical composition and avoiding complexation of interacting ions, it was possible to produce uniform particles of different shapes and internal structures by changing only two physical parameters (pH and ionic strength). Specifically, cubic, prismatic, platelet, and spherical colloidal particles of MgF_2 were formed either by diffusional growth or aggregation of the subunits as classified at the bottom of Figure 1.

The problem with the predictability of final shapes of particles, prepared by precipitation in solutions, becomes even more difficult once the reacting species form various complexes prior to precipitation. It would seem that, at the present state of our understanding of precipitation processes, the formation of uniform spheres is expected when reacting cations hydrolyze and form polymeric solutes which then condense. In contrast, the formation mechanisms of monocrystalline and polycrystalline particles require information on all species in reacting solutions and their interactions, which differ from case to case. Obviously, under such conditions the predictability of the properties of the resulting well-defined solids becomes a rather difficult, if not impossible, task. Rather than being able to predict the formation of a specific dispersions, it is possible to elucidate the formation mechanisms when all relevant data become available.

Acknowledgment. Authors acknowledge Professor D. Goia and Professor V. Privman for fruitful comments. This study was supported by the NSF grant DMR-0509104.

(35) Halaciuga, I.; Goia, D. *J. Mater. Res.* **2008**, *23*, 1776–1784.
(36) Matijević, E.; Goia, D. *Colloids Surf.* **1999**, *146*, 139–152.